Available online at www.sciencedirect.com
SCIENCE DIRECT
Journal of Asian Earth Sciences 28 (2006) 55–62
Journal of Asian Earth Sciences
www.elsevier.com/locate/jaes

Deep resistivity sounding studies in detecting shear zones: A case study from the southern granulite terrain of India

S.B. Singh *, Jimmy Stephen

National Geophysical Research Institute, P.O. Box No. 66, Hyderabad 500 007, India

Received 19 January 2004; received in revised form 3 September 2004; accepted 25 September 2004

Abstract

The resistivity signatures of the major crustal scale shear zones that dissect the southern granulite terrain (SGT) of South India into discrete geological fragments have been investigated. Resistivity structures deduced from deep resistivity sounding measurements acquired with a 10 km long Schlumberger spreads yield significant insights into the resistivity distribution within the E–W trending shear system comprising the Moyar–Bhavani–Salem–Attur shear zone (MBSASZ) and Palghat–Cauvery shear zone (PCSZ). Vertical and lateral extensions of low resistivity features indicate the possible existence of weak zones at different depths throughout the shear zones. The MBSASZ characterized by very low resistivity in its deeper parts (>2500 m), extends towards the south with slightly higher resistivities to encompass the PCSZ. A major resistivity transition between the northern and southern parts is evident in the two-dimensional resistivity images. The northern Archaean granulite terrain exhibits a higher resistivity than the southern Neoproterozoic granulite terrain. Though this resistivity transition is not clear at greater depths, the extension of low resistivity zones has been well manifested. It is speculated here that a network of crustal scale shear zones in the SGT may have influenced the strength of the lithosphere.

Keywords: Deep resistivity sounding; Shear zones; Southern granulite terrain

1. Introduction

The South Indian shield consists of fragments of different crustal blocks joined along or bounded by Proterozoic mobile belts/shear systems. Recently, these crustal scale shear zones in the shield have attracted wide attention owing to their vital role in reconstructing the Precambrian evolution of south India. While geological studies can provide information on the surface manifestations of the shear zones, only geophysical investigations can provide significant depth information, especially regarding the nature and extension of fault zones at different depths. The efficacy of deep resistivity sounding (DRS) studies in investigating the conductive nature of shear zones has been previously reported by Singh et al. (2003), as part of an integrated geophysical/geological investigation of the tectonics of the high grade granulite terrain of South India (Reddy et al., 2000). The associated mineralogy, seismic stresses, fluids, etc. influence the various physical parameters of the shear zones at depth. The N–S trending geo-transect from Kuppam to Palani crosses all the diverse and highly metamorphosed crustal fragments in the SGT. In the present study, we concentrate on the resistivity signatures of the shear systems in the southern part of this Kuppam–Palani geo-transect (Fig. 1). DRS and magnetotelluric sounding (MTS) studies have documented a highly conductive signature for the shear zones, with a steep structure to deep crustal depths (Singh et al., 2003; Harinarayana et al., 2003). The correlation of major shear systems, a large number of deep faults and seismicity with SGT indicate that tectonic activity is continuing (Grady, 1971). A mechanically weakened lithosphere beneath the SGT (Stephen et al., 2003) might have some role in ongoing tectonic processes.

2. Geological setup

The southern granulite terrain of the Indian shield, consisting of exhumed Precambrian lower crust, provides a window for observing ancient crusts reflecting a wide spectrum of metamorphic events within a diverse set of crustal blocks. The SGT contains granite-greenstone rocks in its northern part,

* Corresponding author. Tel.: +91 40 2343 4642; fax: +91 40 2717 1564.
E-mail address: sbsinghji@yahoo.com (S.B. Singh).

1367-9120/$ - see front matter © 2006 Elsevier Ltd. All rights reserved.
doi:10.1016/j.jseaes.2004.09.014

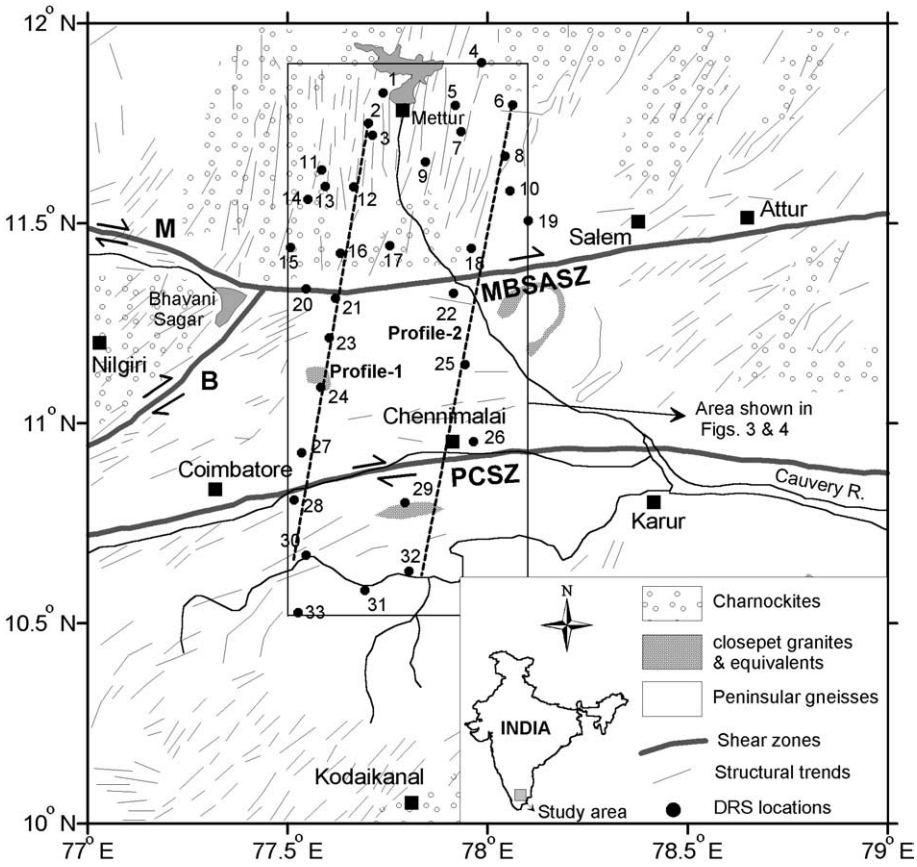

Fig. 1. Deep resistivity sounding (DRS) locations in the southern granulite terrain, superimposed over the geological map showing major shear zones and structural trends (after Ramakrishnan, 2003). PCSZ—Palghat–Cauvery shear zone, MBSASZ—Moyar–Bhavani–Salem–Attur shear zone. The dashed lines show the profiles chosen for making geo-electrical section across the shear zones.

migmatitic gneisses with enclaves of meta-sedimentary and metabasic–ultrabasic rocks in the central region, and dominantly quartzo-feldspathic gneisses with metasedimentary enclaves in the southern parts (Drury et al., 1984). The SGT is separated from the northern granite-greenstone province by a gradational transition with irregular development of charnockites and other granulite facies rocks. This transition is remarkable for its network of Proterozoic shear systems, dividing the terrain into many discrete tectonic blocks (Drury and Holt, 1980). The major shear belt includes the crustal-scale Moyar, Bhavani, Palghat, Cauvery and Attur shear zones, all of which play a key role in reconstructing the Precambrian evolution of South India. Generally, the shear system is E–W trending, dividing geologically different crustal blocks (Raith et al., 1999) (Fig. 1). The Palghat–Cauvery shear zone (PCSZ), exhibits an elongated geometry of about 400×80 km characterized by an E–W aligned tract of intense ductile shearing that is assumed to mark the boundary between the Archaean granulite block in the north and the Neoproterozoic granulite block in the south. The PCSZ is assumed to be the southern margin of the Dharwar Craton (Ramakrishnan, 1993) and the northern margin of Pan-African metamorphism in the south Indian basement (Harris et al., 1994). On the basis of geochronological and P–T estimates, Bhaskar Rao et al. (1996) demonstrates that within the PCSZ the Archaean crustal segment was reworked during the Proterozoic, most intensely during the Neoproterozoic.

The Moyar shear zone, established about 2.5 Ga ago, is marked on either side by high-grade metamorphic rocks, with migmatites in the southwestern Dharwar Craton and high-pressure granulites in the Nilgiri hills (NH). In this shear zone, E–W striking, sub-vertical shear planes truncate structures of the adjacent blocks. Reverse faulting of the southern block implies sub-vertical northward thrusting of the NH some time after the 2.5 Ga-peak of metamorphism (Naha and Srinivasan, 1996). The ENE–WSW striking Bhavani shear zone cuts across the Palaeo-isobars of the NH, indicating that shearing along this tectonic boundary postdates the late Archaean imprint (Raith et al., 1990). Shear indicators and stretching lineation in the Bhavani shear zone reflect oblique-slip movement (Naha and Srinivasan, 1996). On the basis of lithological similarities observed between the Moyar and Bhavani shear zones, Raith et al. (1999) interpret these to be part of one major suture, marking a lithological break with regard to the garnet-bearing enderbites of the adjacent NH. Due to lack of data, the nature and evolution of the Moyar—Bhavani shear belt, which covers an area of more than 12,000 km^2, is still poorly understood. Situated between high-grade crustal blocks, this shear belt is composed of distinct amphibolite facies zones with indicators of intense ductile

shearing and flattening (Meissner et al., 2002). The Salem–Attur shear zone (SASZ) has been accepted as the eastern continuation of MBSZ (Drury et al., 1984; Chetty, 1996; Bhadra, 2000; Jain et al., 2003). In the following discussion, we refer to this shear system as the Moyar–Bhavani–Salem–Attur shear zone (MBSASZ).

3. DRS data and analysis

Lateral and vertical discontinuities in subsurface geoelectrical structures can be delineated by electrical resistivity methods, implemented in profile or sounding modes. The present study makes use of the sounding mode, referred to here as deep resistivity sounding (DRS), to obtain vertical resistivity structures at depths as great as 4–5 km. Good DRS coverage has been obtained for the study area, with a total of 33 stations distributed across the two major shear systems, the MBSZ and the PCSZ. To minimize the influence of lateral inhomogeneities as well as to provide a satisfactory trade off with penetration depth, the four electrode collinear Schlumberger setup was used for all measurements. All 33 soundings were carried out with a maximum current electrode separation (AB or 2L) of 10 km. The distribution of DRS stations is shown in Fig. 1, along with the major shear zones as inferred from photo-geological studies (Drury et al., 1984). Preliminary studies of the sounding curves show complex variations in resistivity throughout the region, with many intermediate low resistive zones at varying depths. The low resistive features at depth in the vicinity of major shear zones may be related to the presence of fluids. Fluid activity is manifested by fluid induced retrograde metamorphism along the major weak zones in SGT (Bhadra, 2000).

The DRS data analysis is based on qualitative and quantitative methods. In the qualitative method, one directly represents variations of resistivity with depth as log–log plots of apparent resistivity against half current electrode separation (Fig. 2). The sounding curves obtained over SGT seems differ from station to station, indicating a highly variable nature for saturated fractures as well as shallow inhomogeneities. For a better qualitative picture, we have also plotted maps of apparent resistivity variation for different current electrode separation (AB/2) in Fig. 3. One-dimensional inversion of the DRS data was carried out using an interactive inversion code, IPI2Win (Bobachev, 2003). IPI2Win provides the opportunity to choose from a set of equivalent solutions and here we choose the one best fitting the geophysical data with least fitting error. The one-dimensional-inverted resistivity models for representative DRS data are shown in Figs. 2 and 4. Fig. 5 shows the

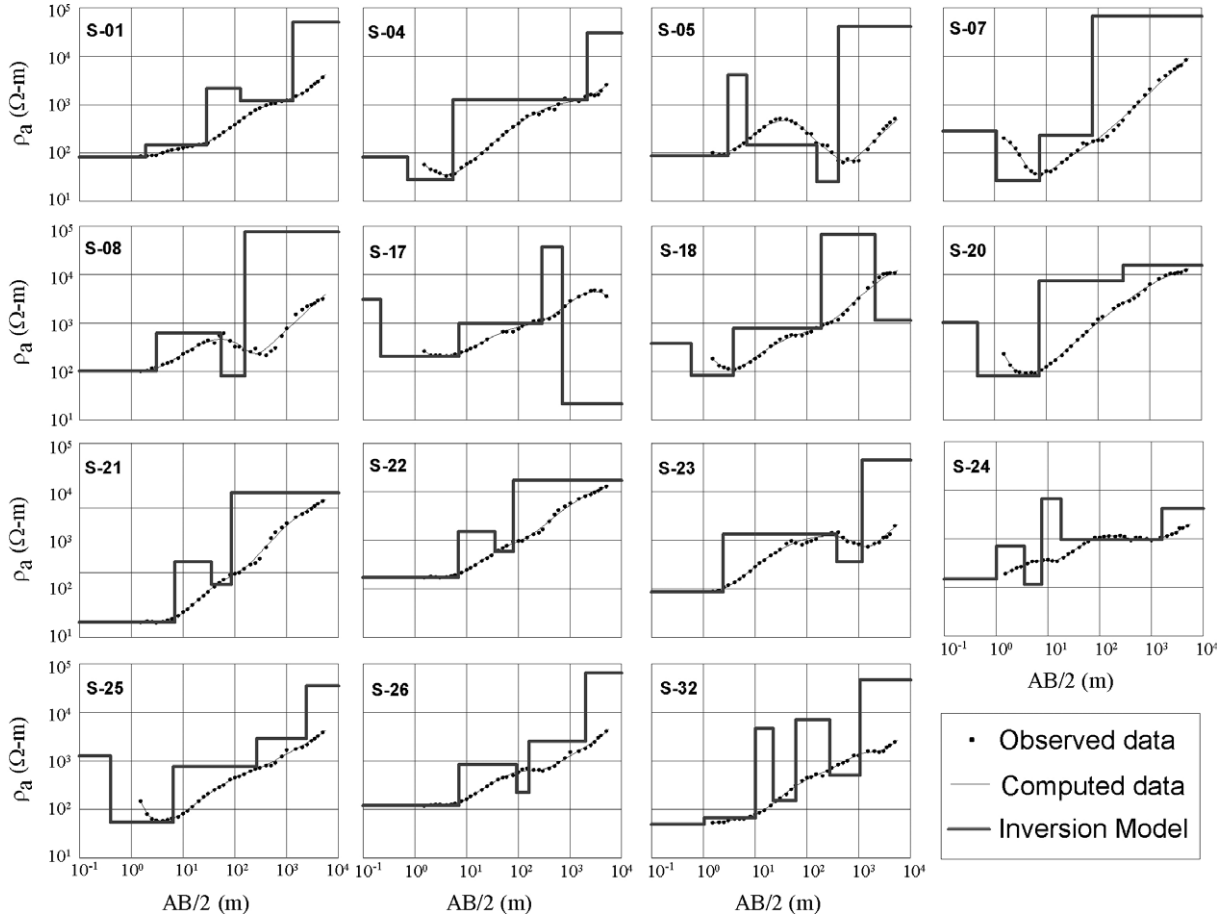

Fig. 2. Selected deep resistivity sounding curves in the study area. The observed and computed curves are shown along with the corresponding inversion models.

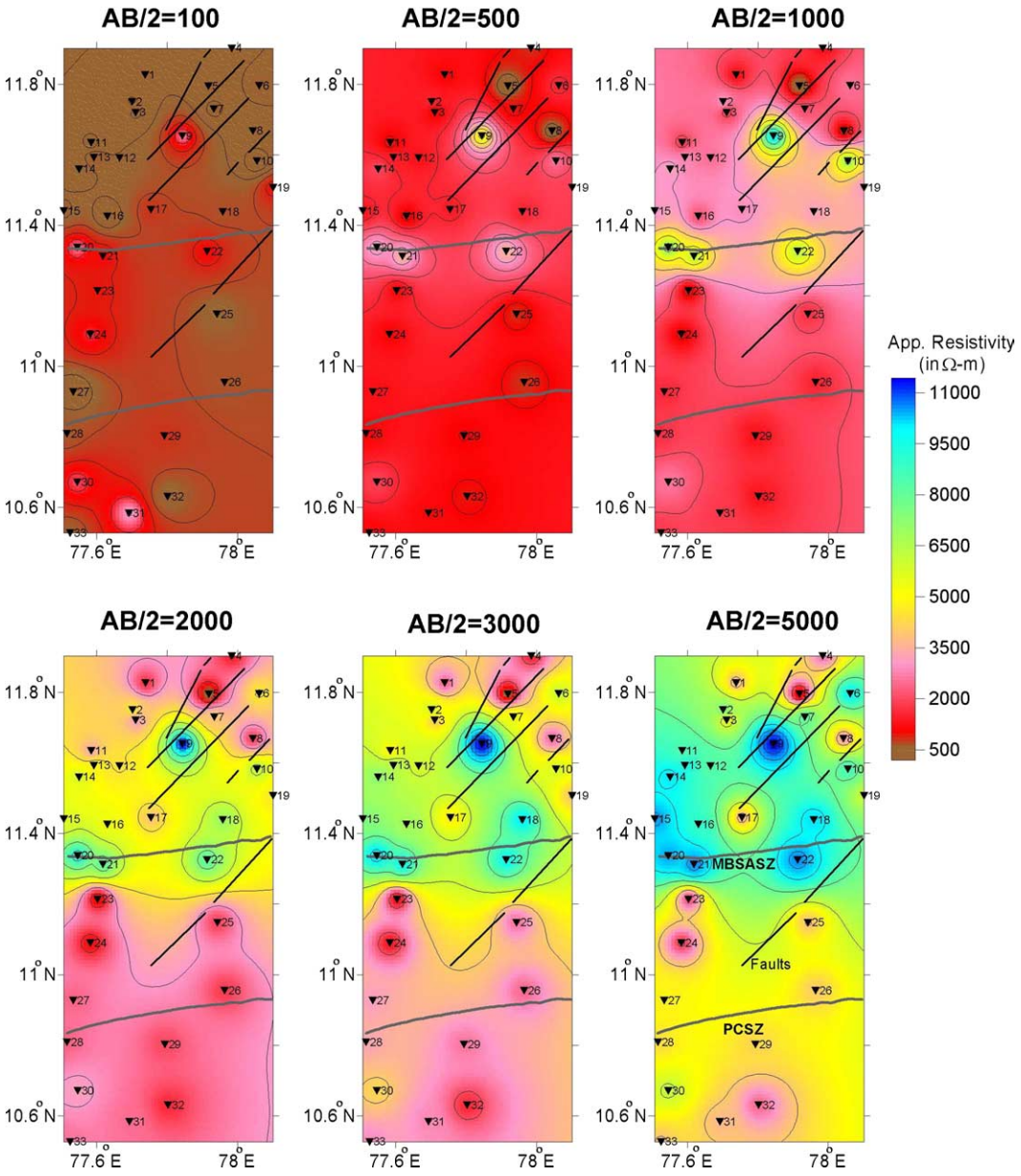

Fig. 3. Apparent resistivity variation observed for different electrode separations (AB/2) in the study area. DRS locations (solid symbols), shear zones (MBSASZ and PCSZ) and the main faults (solid lines) are also shown.

observed (pseudo section for apparent resistivity versus AB/2) and inverted resistivity sections for the two profiles shown in Fig. 1.

4. Results and discussion

Individual DRS curves and their inverted layer models are shown in Fig. 2. Even though the sounding curves appears to be highly variable, low resistivity zones are observed at varying depths at most of the stations. One-dimensional inversion suggests low resistivity zones from 100 s of meter (for example, S-08 and S-26) to greater than 1000 m (for example, S-23 and S-32), and in some regions even deeper (for example, S-17 and to the east S-18). In the northern part of the study area, near Mettur, relatively low resistivities are evident both in the qualitative apparent resistivity image (Fig. 3) and in the one-dimensional inversion (Fig. 2). Apparent resistivity appears to be low for almost all AB/2 in the vicinity of Mettur reservoir as observed in S-01, S-04 and S-05. The deep faults in these region derived from photo-geological studies (Grady, 1971) are also shown in Fig. 3. In spite of the presence of deep faults, the stations other than above three do not show any major low resistivity signatures at large AB/2 separations, suggesting that these faults are not acting as conduits for fluid movement. However, further south towards the MBSASZ, low resistivities at deep levels (e.g. S-17 and S-18) suggest the possible influence of this crustal scale shear system. This eastward extension of a deep low resistivity zone (few 10s of Ohm-meter) supports the earlier suggestions by Chetty (1996) and many others that the SASZ could be the eastern

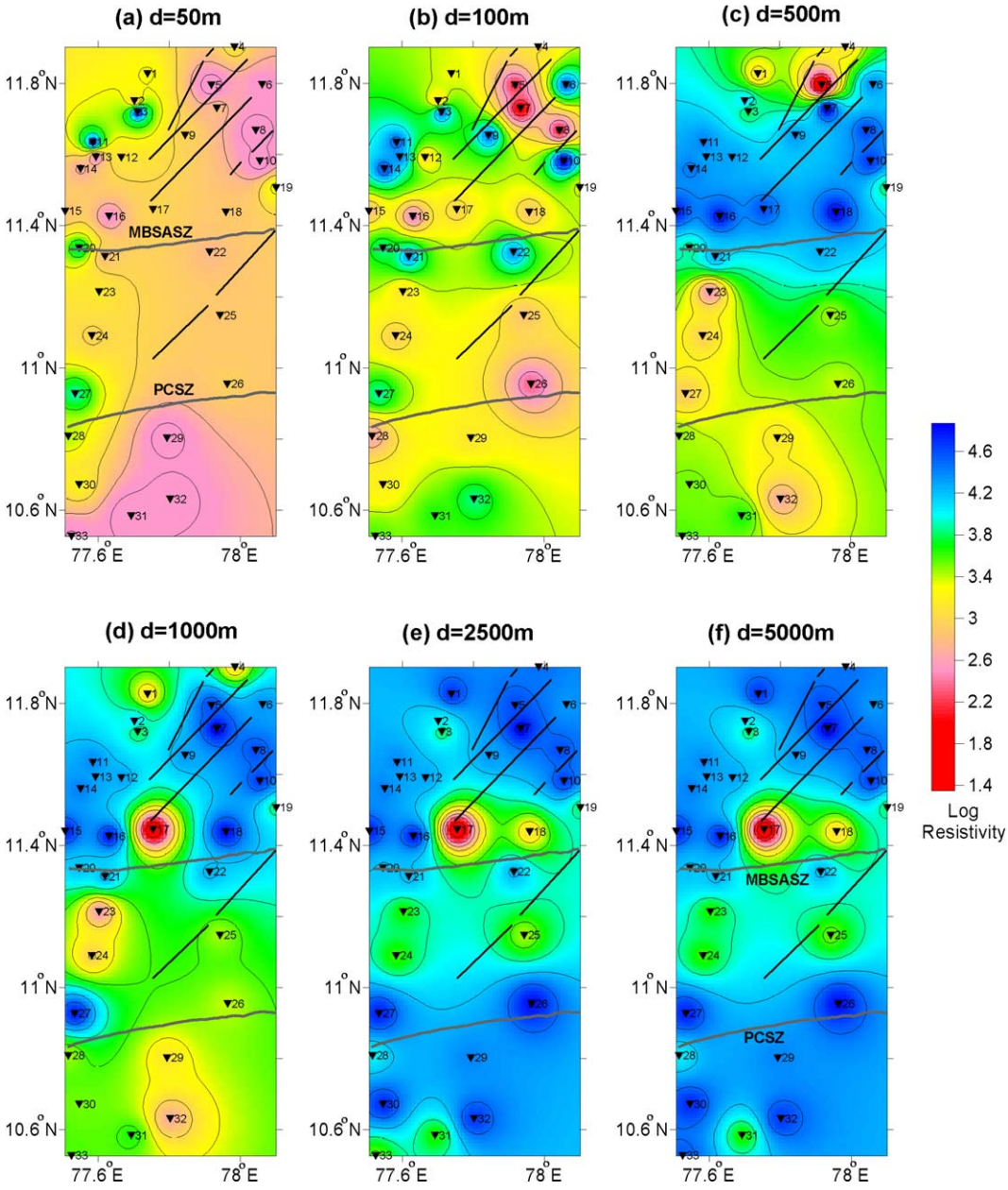

Fig. 4. Resistivity maps at various depths, obtained from one-dimensional inversion of the sounding curves. Resistivities are shown in the logarithmic scale.

continuation of MBSZ. The NE–SW trending (commonly N30°E and N45°E) deep faults identified in these regions (Grady, 1971) may also have some role in controlling the observed low resistivities at depth in discrete pockets.

In contrast to the deep low resistivity features observed north of the MBSASZ (S-17 and S-18), stations immediate to this shear zones (S-20, S-21 and S-22), exhibit a substantially higher resistivity features. However, to the south most of the soundings exhibit low resistivity at intermediate and greater depths. For example, the models obtained for S-24 and S-26 suggest the probable continuation of conductive zones southward. This low resistivity nature further extends to the south of the PCSZ (e.g. S-32). However, compared to the deeper low resistivities observed to the north of MBSASZ (S-17 and S-18), the soundings in southern region do not suggest conductive zones at such great depths. This northward deeper conductive feature may represent a possible north-dipping nature of the MBSASZ. Seismic studies have evidenced northward dipping reflection bands in this region (Reddy et al., 2003).

The apparent resistivity plots give a better qualitative insight into the lateral resistivity variations, though it fails to represent the true resistivities and depths. The apparent resistivity maps in the study region (Fig. 3) clearly shows that there are no prominent features for up to an electrode separation of 500 m. However, at larger separations, a resistive block is clearly evident just north of the PCSZ. The southern boundary of this resistive feature is to the south of MBSASZ and seems to extent further north in all the large electrode separation (AB/2) starting from 1000 m. The present apparent resistivity plots (Fig. 3) demarcate the

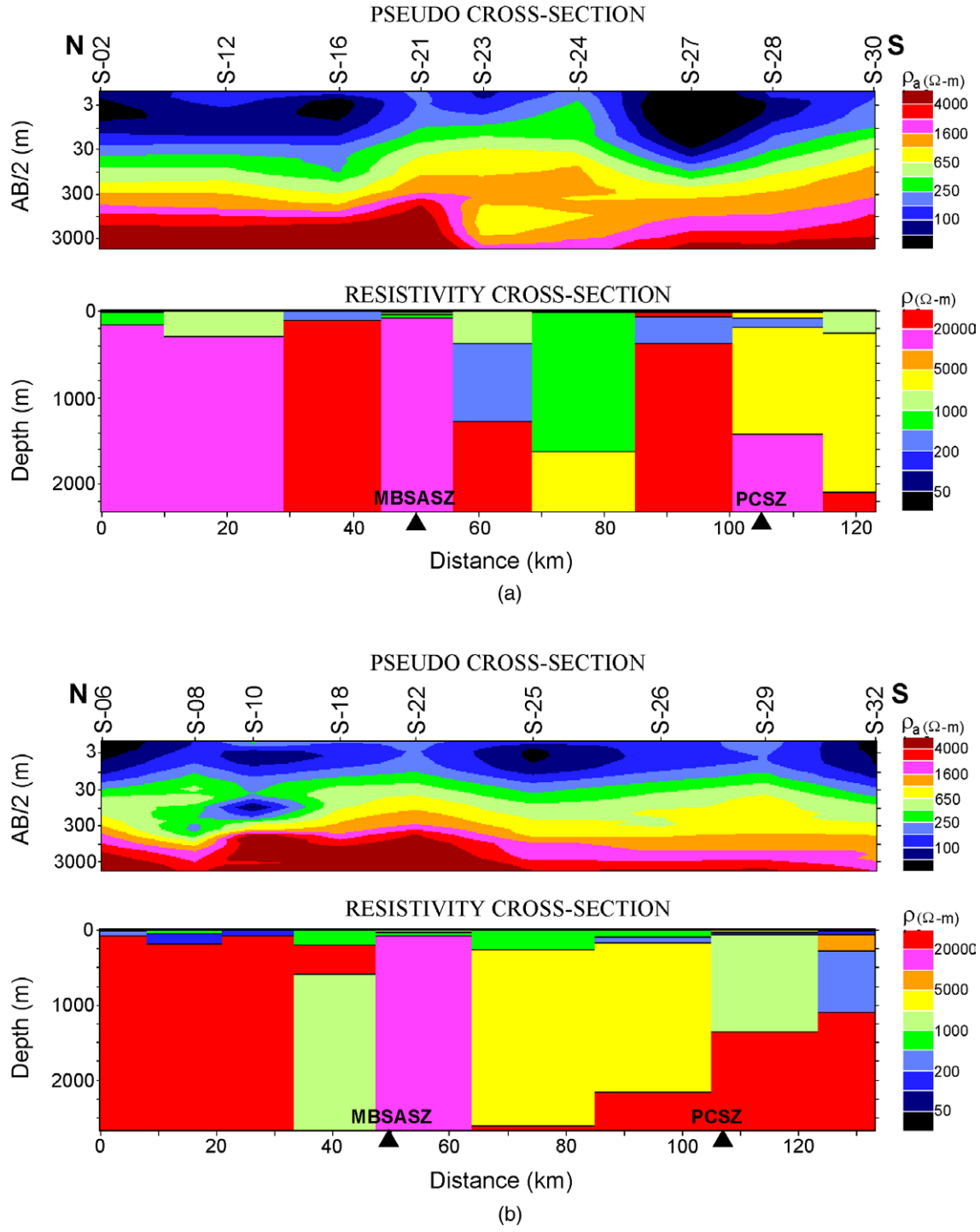

Fig. 5. The pseudo cross-sections and inverted resistivity cross-sections shown for (a) profile-1 and (b) profile-2. The resistivity cross-sections are derived from one-dimensional inversion of the sounding data.

northern high resistivity and southern low resistivity regions. It is assumed that the Archaean terrain towards north of PCSZ exhibits higher resistivity than the southern Pan-African terrain. However, from the map it is clear that the lateral transition from low to high resistivity occurs within the MBSASZ and PCSZ shear system, rather than being exactly at the PCSZ. On the basis of the widespread Pan-African overprint in the retrogressed rocks of the MSZ, Ramakrishnan (2003) suggests the MSZ as the boundary of the northern marginal zone of the Pan-African Pandyan mobile belt. The structural trends in all these shear systems are aligned almost NE–SW or E–W, following the trend of the shear system, in contrast with the general N–S trending structural fabric observed in other regions of South India (see Fig. 1). Quite interestingly, these crustal scale shear systems seem to be influencing the strength of the lithosphere as a

whole. Recent studies by Stephen (2003) show an azimuthal variation in the mechanical strength of the lithosphere, wherein it gets weakened in NE–SW direction almost parallel to the observed structural trends in these shear systems.

Maps of resistivity at different depths ($d=50$, 100, 500, 1000, 2500 and 5000 m) as derived from the one-dimensional inversion are shown in Fig. 4. A logarithmic scale was chosen to minimize the distorted effects of the large range at resistivity values, from few to about 100,000 Ω-m. At a depth of 50 m (Fig. 4a), no features relevant to our present interest are observed; rather an overall low resistivity is present, which diminish with depths. These resistivity variations could be attributed to the uppermost weathered zone as well as common fractures in the bedrock, which control the groundwater movement. Some of the features discussed earlier become evident at depths of 100 m (Fig. 4b). The Mettur region has generally low resistivity, while further west higher resistivities occur. A low/moderate resistivity (<1000 Ω-m) feature trending E–W is observed to the immediate north of MBSASZ. This low resistivity feature follows an E–W trending high resistivity feature to the south of MBSASZ. Further south, a clear low resistivity zone is present, which extends to more than 1000 m depth (Fig. 4d). The resistivity signatures seem to change significantly with depth. The low resistivity and high resistivity E–W trends observed at 100 m in the vicinity of MBSASZ changed. The complex resistivity pattern observed in the northern half of the study area (Fig. 4b) becomes simpler at 500 m depth. The irregular conductive patterns in the north of MBSASZ disappear and reflect a high resistivity nature.

A clear separation of the northern and southern regions of the study area is shown in the resistivity images at 500 m depth. Considering an Archaean–Pan African transition, one could envisage the Archaean rocks possessing a relatively higher resistivity than the Pan-African rocks. Though it is possible to visualize this resistivity distinction to a depth of 1000 m (Fig. 5d), at further depth it is absent. The deeper images (Fig. 4e and f) are more compatible with EW shear systems, showing a low to moderate resistivity trends with this orientation. This central low resistivity zone (comprising S-23, S-24 and S-25) lies within the MBSASZ and PCSZ shear systems. This resistivity trend continues to depths of 2500 m and further. It is expected that the presence of deep faults should also have influenced the deeper low resistivity features to the north of MBSASZ.

The depth variations are further highlighted in the stitched geoelectrical sections obtained from individual one-dimensional inversions of the sounding data carried out along two profiles (profile-1 and profile-2 shown in Fig. 1) across the shear systems (Fig. 5). The sections are shown to a maximum depth of 2750 m. The pseudo cross-section shows the apparent resistivity variation with respect to the current electrode separation (AB/2). It gives the general distribution of conductive and resistive features in a broad way, providing vital information on its lateral extent, though not to the actual depth scale. The inverted resistivity cross-sections depict high resistivity rocks at greater depths, except for a few pockets that discussed earlier (e.g. S-17 and S-18). In general, the association of low resistivity zones at varying depths is observed towards the south of both the profiles. On profile-1, the northern part up to a distance of 50 km (S-21) is uniformly resistive, whereas further south low resistivity features are evident at varying depth levels. Profile-2 also yields a similar picture with a break in the high resistivity zone at a distance of about 60 km. Another low resistivity feature observed in this profile at a distance of 40 km appears to extend to greater depths. Earlier we have seen that the northern boundary of the shear systems (MBSASZ) almost coincides with these resistivity transitions, at distances of about 50–60 km.

The deeper resistivity signatures derived from the wide band magnetotelluric investigations also suggest low resistivity features pertinent to the shear zones and major faults (Harinarayana et al., 2003). They have located many near-vertical conductive features in vicinity of the system of faults (Grady, 1971) and also in both the MBSASZ and PCSZ. Besides, their two-dimensional modeling results provide different deep crustal resistivity in the order 5000 and 1,00,000 Ω-m for the Pan-African and Archaean terrains, respectively, indicating its deeper continuation, which we observed at certain depth levels in our DRS resistivity images (Fig. 4). But any valid correlation between our present results and the MT results are not possible since the latter lack resolution in the DRS depth range and provides much deeper information. Similarly, the deep seismic reflection and refraction studies in this region also provide valuable velocity structures significant to the understanding of the tectonics of this terrain (Reddy et al., 2003). It has been noticed that the southernmost part of the study area shows a northward dipping of the reflection bands. The observed shift in the low to high resistivity terrain boundary to the north of PCSZ in our study may also attribute to this northward dipping.

5. Conclusions

The electrical variation associated with the major shear systems of the MBSASZ and PCSZ in the southern granulite terrain has yielded noteworthy insights on its possible extensions to greater depths. The present study suggests a contingent fact that the resistivity features at depths more than 100 m is influenced by these shear zones, while the resistivity variations observed for the overlying layers reflect the nature of surficial weathering, basement fractures, shallow groundwater movements, etc. The two-dimensional resistivity images depict a significant resistivity transition, clear up to a depth of 1000 m; distinguish the northern Archaean terrain with its relatively higher resistivity from the more conductive southern Pan-African terrain. Our present resistivity images broadly show that the transition occur between these two major shear zones. At depths of about 2500 m and greater, the resistivity distribution depicts the shear system as a low resistivity zone compared to the surroundings (Fig. 4e and f). The high resistivity features observed within this shear system may be attributed to the occurrence of Archaean Supracrustals (Drury et al., 1984). Beneath the MBSASZ, more conductive features are obtained at deeper portions. The low resistivity features

observed at greater depths could suggest the possible extension of these shear zones to such depths in the SGT.

Acknowledgements

The authors sincerely thank Profs Larry Brown and B. R. Arora for their constructive review comments and Dr K.V. Wilbert Kehelpannala for his suggestions that helped to significantly improve this paper. Dr V. P. Dimri, Director, NGRI is acknowledged for granting permission to publish this paper. DST, New Delhi is acknowledged for its project support and thanks to DRS project team for field investigations.

References

Bhadra, B.K., 2000. Ductile shearing in Attur shear zone and its relation with Moyar shear zone, south India. Gondwana Res. 3, 361–370.

Bhaskar Rao, Y.J., Chetty, T.R.K., Janardhan, A.S., Gopalan, K., 1996. Sm–Nd and Rb–Sr ages and P–T history of the Archaean Sittampundi and Bhavani layered complexes in the Cauvery shear zone, south India: evidence for Neoproterozoic reworking of Archaean crust. Contrib. Mineral. Petrol. 125, 237–250.

Bobachev, A., 2003. IPI2Win—1D automatic and manual interpretation software for VES data, Available online: geophys.geol.msu.ru/ipi2win.htm

Chetty, T.R.K., 1996. Proterozoic shear zones in southern granulite terrain, India. Gond. Res. Group Mem. 3, 77–89.

Drury, S.A., Holt, R.W., 1980. The tectonic framework of south Indian Craton: a reconnaissance involving Landsat Imagery. Tectonophysics 65, T1–T15.

Drury, S.A., Harris, N.B.W., Holt, R.W., Reeves-Smith, G.J., Wightman, R.T., 1984. Precambrian tectonics and crustal evolution in South India. J. Geophys. 92, 3–20.

Grady, J.C., 1971. Deep main faults in south India. J. Geol. Soc. India. 17, 56–62.

Harinarayana, T., Naganjaneyulu, K., Manoj, C., Patro, B.P.K., Begum, S.K., Murthy, D.N., Rao, M., Kumaraswamy, V.T.C., Virupakshi, G., 2003. Magnetotelluric investigations along Kuppam-Palani geotransect, south India—2D modeling results. Mem. Geol. Soc. India 50, 107–124.

Harris, N.B.W., Santosh, M., Taylor, P.N., 1994. Crustal evolution in south India, constraints from Nd isotopes. J. Geol. 102, 139–150.

Jain, A.K., Singh, S., Manickavasagam, R.M., 2003. Intracontinental shear zones in the southern granulite terrain: their kinematics and evolution. Mem. Geol. Soc. India 50, 225–253.

Meissner, B., Deters, P., Srikantappa, C., Kohler, H., 2002. Geochronological evolution of the Moyar, Bhavani and Palghat shear zones of southern India: implications for east Gondwana correlations. Precambrian Res. 114, 149–175.

Naha, K., Srinivasan, R., 1996. Nature of the Moyar and Bhavani shear zones, with a note on its implications on the tectonics of the southern Indian Precambrian shield. Proc. Indian Acad. Sci. (Earth Planet. Sci.) 105, 143–189.

Raith, M., Srikantappa, C., Ashamanjari, K.G., Spiering, B., 1990. The granulite terrane of the Nilgiri Hills (south India): characterization of high-grade metamorphism. In: Vielzeuf, D., Vidal, P.H. (Eds.), Granulites and Crustal Evolution. pp. 339–365.

Raith, M., Srikantappa, C., Buhl, D., Kohler, H., 1999. The Nilgiri enderbites, south India: nature and age constraints on protolith formation, high-grade metamorphism and cooling history. Precambrian Res. 98, 129–150.

Ramakrishnan, M., 1993. Tectonic evolution of the granulite terrains of southern India. Mem. Geol. Soc. India 25, 35–44.

Ramakrishnan, M., 2003. Craton-Mobile Belt relations in southern granulite terrain. Mem. Geol. Soc. India 50, 1–24.

Reddy, P.R., Mishra, D.C., Sarma, S.V.S., Harinarayana, T., Divakara Rao, V., Narayana, B.L., Singh, S.B., 2000. Subsurface configuration of the southern high grade granulite terrain—inferences from integrated geological/geochemical/seismic/magnetotelluric/deep resistivity and gravity studies. Indian Mineral. 34, 41–47.

Reddy, P.R., Rajendra Prasad, B., Rao, V.V., Sain, K., Rao, P.P., Khare, P., Reddy, M.S., 2003. Deep seismic reflection and refraction / wide-angle reflection studies along Kuppam–Palani transect in the southern granulite terrain of India. Mem. Geol. Soc. India 50, 79–106.

Singh, S.B., Stephen, J., Singh, U.K., Srinivas, Y., Ashok Babu, G., Singh, K.P., Janna Reddy, E., 2003. Electrical signatures in the high grade metamorphic terrain of south India using deep resistivity sounding studies. Mem. Geol. Soc. India 50, 125–138.

Stephen, J., 2003. South Indian shield lithosphere: its mechanical strength and anisotropy. PhD Thesis, SRTM University, Nanded, India.

Stephen, J., Singh, S.B., Yedekar, D.B., 2003. Elastic thickness and isostatic coherence anisotropy in the south Indian Peninsular Shield and its implications. Geophys. Res. Lett. 30 (16), 1853. doi:10.1029/2003GL017686.